Glycobiology vol. 19 no. 2 pp. 126–134, 2009
doi:10.1093/glycob/cwn110
Advance Access publication on October 24, 2008

The *N*-linked oligosaccharide at FcγRIIIa Asn-45: an inhibitory element for high FcγRIIIa binding affinity to IgG glycoforms lacking core fucosylation

Mami Shibata-Koyama[2], Shigeru Iida[2], Akira Okazaki[2], Katsuhiro Mori[2], Kazuko Kitajima-Miyama[2], Seiji Saitou[2], Shingo Kakita[2], Yutaka Kanda[2], Kenya Shitara[2], Koichi Kato[3,4], and Mitsuo Satoh[1,2]

[2]Tokyo Research Laboratories, Kyowa Hakko Kogyo Co., Ltd, 3-6-6 Asahi-machi, Machida-shi, Tokyo 194-8533; [3]Graduate School of Pharmaceutical Sciences, Nagoya City University, Mizuho-ku, Nagoya 467-8603; and [4]Okazaki Institute for Integrative Bioscience and Institute for Molecular Science, National Institutes of Natural Sciences, 5-1 Higashiyama, Myodaiji, Okazaki, Aichi 444-8787, Japan

Received on August 22, 2008; revised on October 9, 2008; accepted on October 10, 2008

Human leukocyte receptor IIIa (FcγRIIIa) plays an important role in mediating therapeutic antibodies' antibody-dependent cellular cytotoxicity (ADCC), which is closely related to the clinical efficacy of anticancer processes in humans *in vivo*. The removal of the core fucose from oligosaccharides attached to the Fc region of antibodies improves FcγRIIIa binding, allowing the antibodies to enhance dramatically the antibody effector functions of ADCC. In this study, the contribution of FcγRIIIa oligosaccharides to the strength of the FcγRIIIa/antibody complex was analyzed using a serial set of soluble human recombinant FcγRIIIa lacking the oligosaccharides. A nonfucosylated antibody IgG1 appeared to have a significantly higher affinity to the wild-type FcγRIIIa fully glycosylated at its five *N*-linked oligosaccharide sites than did the fucosylated IgG1, and this increased binding was almost abolished once all of the FcγRIIIa glycosylation was removed. Our gain-of-function analysis in the FcγRIIIa oligosaccharide at Asn-162 (N-162) confirmed that N-162 is the element required for the high binding affinity to nonfucosylated antibodies, as previously revealed by loss-of-function analyses. Interestingly, beyond our expectation, the FcγRIIIa modified by N-162 alone showed a significantly higher binding affinity to nonfucosylated IgG1 than did the wild-type FcγRIIIa. Attachment of the other four oligosaccharides, especially the FcγRIIIa oligosaccharide at Asn-45 (N-45), hindered the high binding affinity of FcγRIIIa to nonfucosylated IgG1. Our data clearly demonstrated that N-45 is an inhibitory element for the high FcγRIIIa binding affinity mediated by N-162 to nonfucosylated antibodies. This information can be exploited for the structural-based functional study of FcγRIIIa.

Keywords: FcγRIIIa Asn-45/FcγRIIIa binding affinity/IgG1 lacking core fucosylation/*N*-linked Fc oligosaccharides/*N*-linked FcγRIIIa oligosaccharides

Introduction

Most therapeutic antibodies that have been licensed and developed as medical agents are of the human IgG1 isotype. Human IgG1 is a heavily fucosylated glycoprotein bearing two *N*-linked biantennary complex-type oligosaccharides bound to the antibody constant region (Fc) via Asn-297, and it exercises biological activities referred to as "effector functions" of antibody-dependent cellular cytotoxicity (ADCC) and complement-dependent cytotoxicity (CDC) through the interaction of the Fc with either leukocyte receptors (FcγRs) or complement components. Genetic analyses of FcγR polymorphisms of cancer patients have demonstrated that ADCC is one of the major critical mechanisms responsible for the clinical efficacy of therapeutic antibodies such as anti-CD20 rituximab (Rituxan®) and anti-Her2 trastuzumab (Herceptin®) (Cartron et al. 2002; Weng and Levy 2003; Dall'Ozzo et al. 2004; Gennari et al. 2004; Kim et al. 2006). For patients carrying the high-affinity FcγRIIIa allotype (FcγRIIIa-Val-158), in contrast to those carrying the low-affinity allotype (FcγRIIIa-Phe-158), superior clinical responses have also been demonstrated in cases such as rituximab-treated systemic lupus erythematosus (SLE) and Waldenstrom's macroglobulinemia, Crohn's disease treatment with anti-TNF-α infliximab (Remicade®), and pregnant women with fetal hemolytic disease treated with anti-RhD (Anolik et al. 2003; Louis et al. 2004; Miescher et al. 2004; Treon et al. 2005). Thus, the importance of ADCC for the clinical efficacy of therapeutic antibodies is now widely recognized.

Interestingly, the Fc oligosaccharide structures of therapeutic antibodies greatly influence FcγRIIIa binding, and the removal of the core fucose from Fc oligosaccharides dramatically enhances the effector functions of ADCC via improved FcγRIIIa binding both *in vitro* and *in vivo* (Shields et al. 2002; Shinkawa et al. 2003; Niwa, Hatanaka, et al. 2004; Niwa, Shoji-Hosaka, et al. 2004; Yamane-Ohnuki et al. 2004; Niwa et al. 2005; Iida et al. 2006; Kanda et al. 2006; Satoh et al. 2006; Suzuki et al. 2007). Although fucose depletion from the Fc oligosaccharides of antibodies is found to improve binding affinity to FcγRIIIa via an enthalpy-driven and association-rate-assisted mechanism (Okazaki et al. 2004), the precise, structurally based mechanisms of the affinity enhancement remain to be elucidated. In the FcγRIIIa/IgG complexes, the interaction sites on the Fc for binding to FcγRIIIa form protein portions in the hinge and C_H2 regions only (Morgan et al. 1995; Clark 1997). The generation of the essential Fc tertiary conformation for binding to FcγRIIIa depends on the presence of the Fc oligosaccharides attached to the C_H2 domains, and the antibody effector functions mediated via FcγRIIIa are severely abrogated in aglycosylated forms of antibodies (Tao and Morrison 1989; Krapp et al. 2003). The crystal

[1]To whom correspondence should be addressed: Tel: +81-42-725-2556; Fax: +81-42-726-8330; e-mail: msatoh@kyowa.co.jp

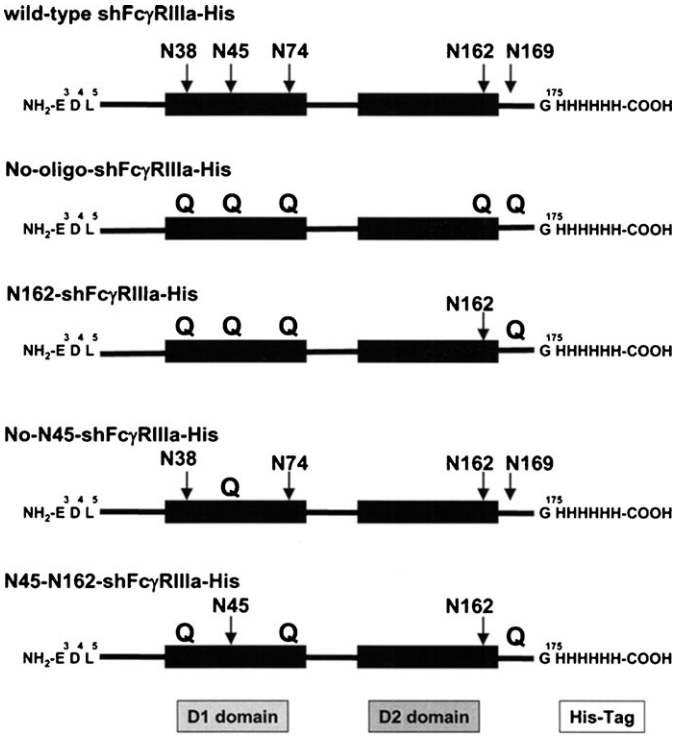

Fig. 1. Structures of soluble human recombinant FcγRIIIa proteins. Schematic structures of the hexa-His-tagged soluble human recombinant FcγRIIIa (shFcγRIIIa-His) lacking the *N*-linked oligosaccharides we expressed in this study are illustrated. Arrows indicate the *N*-glycosylation sites of each shFcγRIIIa-His, and *Q*s represent altering asparagine of *N*-linked glycosylation sites into glutamine to delete the glycosylation.

structure analysis of human IgG1 has revealed that the antibody oligosaccharides linked to the Fc are integral to the protein portion of the Fc and form multiple noncovalent interactions with the C_H2 domains (Huber et al. 1976; Harris et al. 1998; Radaev et al. 2001). Thus, multiple noncovalent interactions between the oligosaccharides and the protein exert a reciprocal influence of each on the conformation of the other, and these complexities of human IgG1, along with the core fucose heterogeneity of the Fc oligosaccharides, delicately affect the binding affinity with FcγRIIIa.

Human FcγRIIIa is also a glycoprotein bearing five *N*-linked oligosaccharides bound to the asparagine residues at positions 38, 45, 74, 162, and 169 (Ravetch and Perussia 1989). Recently, based on the crystal structure analysis, the ADCC enhancement by IgG1 lacking core fucosylation was attributed to a subtle conformational change in a limited region of the Fc of IgG1 (Matsumiya et al. 2007), and the high affinity of nonfucosylated antibodies for FcγRIIIa is partially mediated by interactions formed between the FcγRIIIa oligosaccharide at Asn-162 and regions of the Fc that are only accessible when the Fc oligosaccharides are nonfucosylated (Ferrara et al. 2006). In this study, we focused on the FcγRIIIa oligosaccharides to elucidate their functions in the complex interaction between FcγRIIIa and IgG1 antibody molecules more precisely. The results give us new and important insights for better understanding the efficacy of antibody therapies, especially therapeutic antibodies lacking core fucosylation.

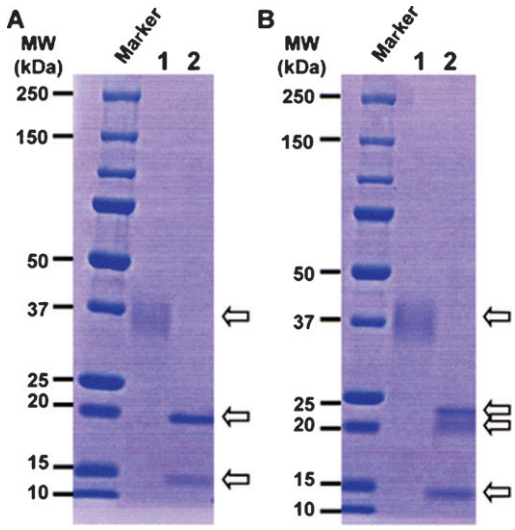

Fig. 2. SDS-PAGE of the shFcγRIIIa-His purified by Ni-NTA chromatography. The expressed products of shFcγRIIIa-His were purified from the culture medium by Ni-NTA chromatography and subjected to nonreducing (**A**) and reducing (**B**) 5–20% SDS–PAGE analyses. Lane 1: the wild-type shFcγRIIIa-His (1 μg), lane 2: N162-shFcγRIIIa-His (1 μg).

Results

Purification of N-linked oligosaccharide-depleted FcγRIIIa

A serial set of the hexa-His-tagged soluble human recombinant FcγRIIIa (shFcγRIIIa-His) lacking the *N*-linked oligosaccharides was generated by altering asparagine of the *N*-glycosylation sites into glutamine using the wild-type FcγRIIIa-Val-158 bearing five *N*-linked glycosylation sites as a template. These included shFcγRIIIa-His lacking all five *N*-linked oligosaccharides (No-oligo-shFcγRIIIa-His), shFcγRIIIa-His bearing only one oligosaccharide at Asn-162 (N162-shFcγRIIIa-His), shFcγRIIIa-His bearing oligosaccharides at both Asn-45 and Asn-162 (N45-N162-shFcγRIIIa-His), shFcγRIIIa-His lacking only one oligosaccharide at Asn-45 (No-N45-shFcγRIIIa-His), and the wild-type shFcγRIIIa-His bearing all five *N*-linked oligosaccharides (Figure 1). The N-terminal amino acid of these shFcγRIIIa-His proteins was unified to Glu^3 by directly connecting to a signal peptide to avoid the N-terminal amino acid heterogeneity observed in the expression of original FcγRIIIa cDNA. The mammalian expression vector carrying each cDNA for the wild-type and mutants was introduced into Chinese hamster ovary (CHO) cell line CHO/DG44, and the expressed products were purified from the culture medium by Ni-NTA chromatography. The wild-type shFcγRIIIa-His migrated as a broadband of a glycoprotein with the appropriate molecular weight of about 37 kDa (Figure 2, lane 1). In the expression of N162-shFcγRIIIa-His, degraded products were observed (Figure 2, lane 2), and the N-terminal amino acid sequence analysis revealed that the lowest SDS–PAGE band under the reducing condition contained the four degraded products whose N-terminal amino acid sequences were Glu^3-Asp-Leu-Lys-Pro-Lys-Ala-Val-Val-Phe-Leu^{13}, Lys^{131}-Tyr-Phe-His-His-Asn^{136}, Ala^{144}-Thr-Leu-Lys-Asp-Ser-Gly-Ser-Tyr^{152}, and Asp^{148}-Ser-Gly-Ser-Tyr-Phe^{153} (Figure 3). The N-terminal amino acid sequence of the highest

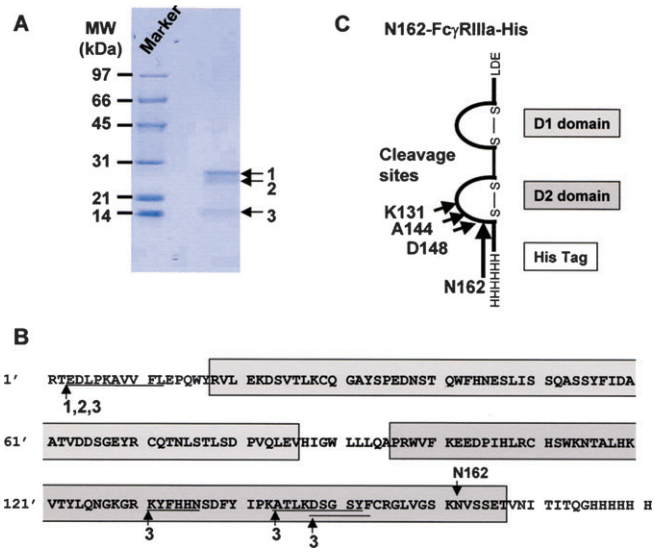

Fig. 3. Degradation of N162-shFcγRIIIa-His. The expressed products of N162-shFcγRIIIa-His (10 μg) purified from the culture medium by Ni-NTA chromatography were subjected to reducing 12% SDS–PAGE (**A**). The N-terminal amino acid sequences of the three detected bands indicated as arrows were analyzed by the Edman degradation method (**B**). The cleavage sites are shown in the schematic model of N162-shFγRIIIa-His (**C**).

and middle bands was Glu[3]-Asp-Leu-Lys-Pro-Lys-Ala-Val-Val-Phe-Leu[13] (Figure 3). This degradation was not inhibited even though the culture medium was prepared in the presence of protease inhibitors including 0.5 mM PMSF, 3.6 μM pepstatin A, 0.3 μM aprotinin, 16.1 μM bestatin, 5.6 μM E-64, and 4.6 μM leupeptin. Comparable degraded products were also observed in No-oligo-shFcγRIIIa-His, although no such degraded product was observed among the other three shFcγRIIIa-His recombinants (data not shown). Subsequent gel filtration chromatography excluded the degraded products to yield almost homogeneously purified (over 95%) products in SDS–PAGE analysis under the nonreducing condition (Figure 4A). All purified shFcγRIIIa-His products migrated as bands with almost the same sizes as we had expected in SDS–PAGE (Figure 4).

Characterization of N-linked oligosaccharide-depleted FcγRIIIa

SDS–PAGE analysis under the reducing condition revealed that two purified samples, that of No-oligo-shFcγRIIIa-His and that of N162-shFcγRIIIa-His, each still contained a band with a lower molecular weight than the expected products, which was observed in the products purified by Ni-NTA chromatography (Figure 4B). Interestingly, IgG affinity chromatography analysis showed that the band retained the ability to bind IgG1 (Figure 5). The majority of the attached oligosaccharides of N162-shFcγRIIIa-His were of the sialylated biantennary complex-type oligosaccharides containing two galactoses with a fucosylated core structure, and the nonsialylated neutral oligosaccharide form was a minor component of the oligosaccharides attached to N162-shFcγRIIIa-His (Figure 6). The oligosaccharide structure of the wild type and other shFcγRIIIa-His mutants produced by CHO/DG44 was confirmed to be of the complex type (data not shown).

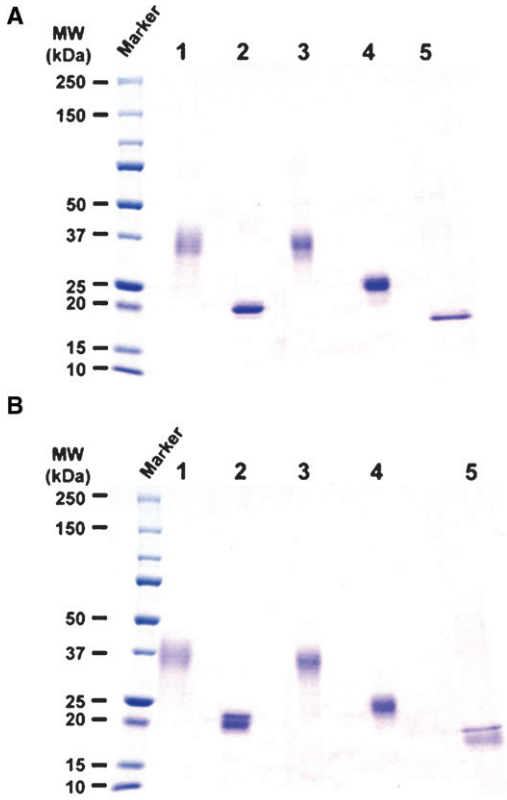

Fig. 4. SDS–PAGE of the purified shFcγRIIIa-His. Each sample (3 μg) of the purified shFcγRIIIa-His produced by CHO/DG44 was subjected to nonreducing (**A**) and reducing (**B**) 5–20% SDS–PAGE. Lane 1: the wild-type shFcγRIIIa-His, lane 2: N162-shFcγRIIIa-His, lane 3: No-N45-shFcγRIIIa-His, lane 4: N45-N162-shFcγRIIIa-His, lane 5: No-oligo-shFcγRIIIa-His.

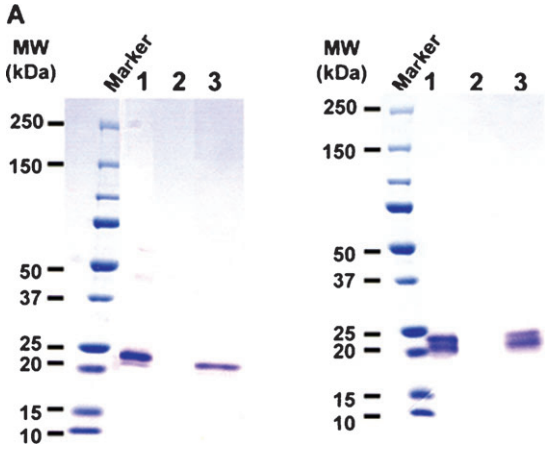

Fig. 5. Binding activity of N162-shFcγRIIIa-His to IgG1. The purified N162-shFcγRIIIa-His was loaded onto a column of nonfucosylated IgG1-immobilized Sepharose. The fractions of load (lane 1), flowthrough (lane 2), and elution (lane 3) were subjected to nonreducing (**A**) and reducing (**B**) 5–20% SDS–PAGE. No detectable protein was observed in the flowthrough fraction, and the whole flowthrough fraction was concentrated to apply SDS–PAGE.

IgG1 binding activity

The IgG1 binding activity of the wild-type and of each purified mutant shFcγRIIIa lacking the *N*-linked oligosaccharides

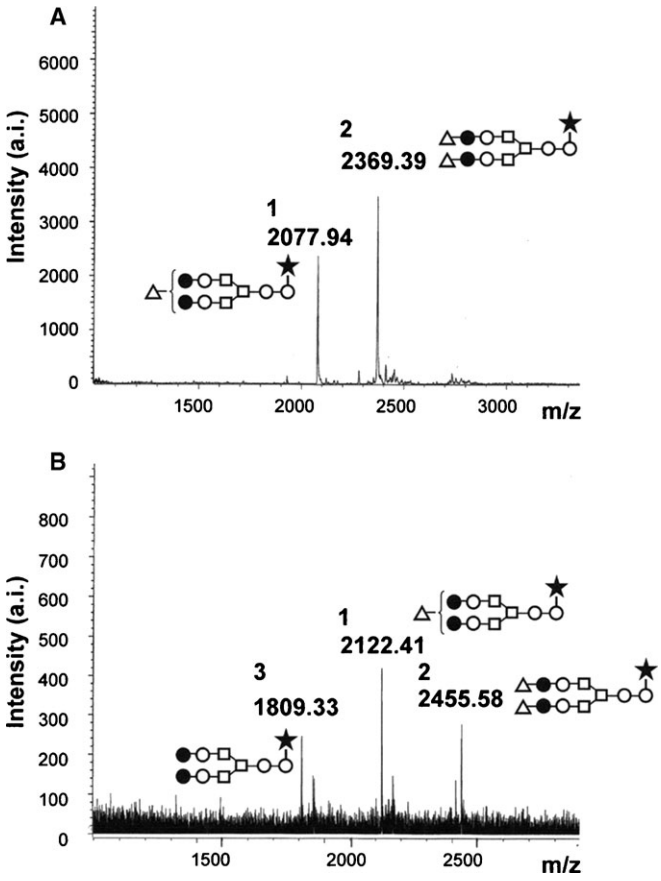

Fig. 6. MALDI-TOF MS spectra of oligosaccharides from N162-shFcγRIIIa-His. Oligosaccharides released from N162-shFcγRIIIa-His by PNGase F digestion were analyzed using a MALDI-TOF MS spectrometer Reflex III in both a negative-ion mode (**A**) and a positive-ion mode (**B**). The *m/z* value corresponds to the sodium-associated oligosaccharide ion. The schematic oligosaccharide structures of each peak (1, 2, and 3) are illustrated: GlcNAc (open circles), mannose (open squares), galactose (closed circles), sialic acid (open triangles), and fucose (closed stars).

was estimated by FcγRIIIa-binding ELISA and by surface plasmon resonance measurement using shFcγRIIIa-His. Compared with the binding to fucosylated IgG1, the wild-type FcγRIIIa showed superior binding affinity to nonfucosylated IgG1. This phenomenon was also observed in the three FcγRIIIa mutants lacking the *N*-linked oligosaccharides except for the FcγRIIIa mutant lacking all five *N*-linked oligosaccharides of No-oligo-shFcγRIIIa-His (Figure 7). No-oligo-shFcγRIIIa-His showed mostly equivalent binding to IgG1 irrespective of core fucosylation and weaker binding than the other glycosylated FcγRIIIas to nonfucosylated IgG1. A binding kinetics analysis using a BIAcore™ biosensor system T100 (BIAcore, Uppsala, Sweden) confirmed the differences observed in FcγRIIIa-binding ELISA (Figure 8). The sensorgrams clearly showed that N162-shFcγRIIIa-His carrying only one *N*-linked oligosaccharide at Asn-162 had the strongest binding affinity to nonfucosylated IgG1 rather than the wild-type shFcγRIIIa-His (Figure 8B and F) and that the additional attachment of *N*-linked oligosaccharide at Asn-45 decreased the high binding affinity (Figure 8F and G). The deletion of the *N*-linked oligosaccharide at Asn-45 in the wild-type shFcγRIIIa-His also exhibited its negative effect on the binding affinity to nonfucosylated IgG1 to increase the binding affinity of No-N45-shFcγRIIIa-His (Figure 8B and H). N45-N162-shFcγRIIIa-His carrying two *N*-linked oligosaccharides at Asn-45 and Asn-162 showed higher binding affinity to nonfucosylated IgG1 than the wild-type shFcγRIIIa-His having three more *N*-linked oligosaccharides (Figure 8B and G). The FcγRIIIa mutant lacking all five *N*-linked oligosaccharides of No-oligo-shFcγRIIIa-His had the weakest binding affinity to nonfucosylated IgG1 among all tested shFcγRIIIa-His (Figure 8D). The interaction of fucosylated IgG1 with FcγRIIIa was not as strong as that observed between nonfucosylated IgG1 and FcγRIIIa as a whole. The affinity of N162-shFcγRIIIa-His to fucosylated IgG1 was slightly weaker than that of No-oligo-shFcγRIIIa-His, and N45-N162-shFcγRIIIa-His showed the weakest affinity to fucosylated IgG1.

Discussion

Recently, ADCC enhancement technology has been expected to play key roles in improving the efficacy of current therapeutic antibodies, especially anticancer antibodies. Enhancement of the binding of therapeutic antibodies for FcγRIIIa has received considerable attention for the development of next-generation therapeutic antibodies with the improved clinical efficacy of ADCC. Indeed, several clinical trials using such therapeutics are ongoing. To understand the physiological functions and to examine in detail the efficacy of these new types of therapies *in vivo*, it is very important to understand the interactions between the therapeutics and the target molecule for the effector functions. Thus, in this study, we focused on the interaction between FcγRIIIa and therapeutic antibodies, especially on the effects of the FcγRIIIa oligosaccharides on the high binding affinity of FcγRIIIa to IgG1 lacking core fucosylation.

FcγRIIIa of mammalian origin is well known as a highly glycosylated protein with five *N*-linked glycosylation sites. However, only a few observations are available on the influences of the FcγRIIIa oligosaccharides on the functions of FcγRIIIa, namely, monomeric fucosylated IgG binds to FcγRIIIa lacking the *N*-linked oligosaccharide at Asn-162 with higher affinity than to the wild-type FcγRIIIa (Ferrara et al. 2006). This finding has also been reported in the loss-of-function analysis of FcγRIIIb, the highly homologous FcγR having the oligosaccharide at the same position as FcγRIIIa, by means of prokaryotic expression, glycosylation site mutation, and tunicamysin-treatment glycosylation depletion in mammalian cell expression (Galon et al. 1997; Drescher et al. 2003). In this study, first we found that it is hard to stably express aglycosylated FcγRIIIa without any degradation by mammalian CHO/DG44 cells as host cells (Figure 2). This degradation seemed to be caused by some intracellular event(s) because the exogenous addition of protease inhibitors, including PMSF, pepstatin A, aprotinin, bestatin, E-64, and leupeptin, into culture medium did not affect the phenomenon. FcγRIIIa carrying just one *N*-linked oligosaccharide at Asn-162 (N-162) was also degraded when expressed in mammalian CHO/DG44 cells, as was aglycosylated FcγRIIIa. The cleavage sites were located in a lysine and arginine cluster region of the FcγRIIIa D2 domain, and the cathepsin-like proteases appeared to be responsible for the cleavages (Figure 3). Interestingly, this degradation was not

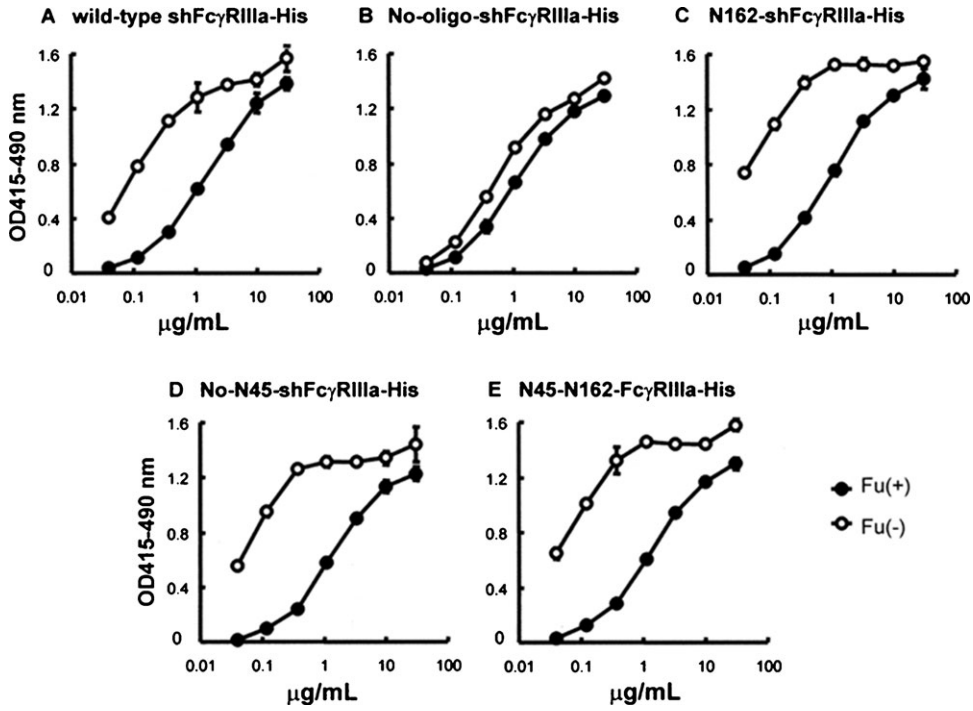

Fig. 7. ELISA binding activity of shFcγRIIIa-His to IgG1. Each variant of shFcγRIIIa-His (the wild-type shFcγRIIIa-His (**A**), No-oligo-shFcγRIIIa-His (**B**), N162-shFcγRIIIa-His (**C**), No-N45-shFcγRIIIa-His (**D**), and N45-N162-shFcγRIIIa-His (**E**)) was coated on 96-well immunoplates using anti-tetra-His antibodies, and the plates were incubated with the indicated concentration of nonfucosylated (Fu(−) (○)) and fucosylated (Fu(+) (●)) anti-CD20 IgG1s. Binding was detected by peroxidase-labeled goat anti-human IgG1 polyclonal antibodies for a 10-min reaction. The mean values ± SD are shown.

observed in the FcγRIIIa carrying N-162 and one more *N*-linked oligosaccharide at Asn-45 (N-45), which means that the attachment of N-45 to the FcγRIIIa D1 domain affects the D2 domain protease sensitivity despite the different domain location. The N-45 attachment in the D1 domain might cause a conformational change of FcγRIIIa to further stabilize the D2 domain structure.

We succeed in removing the degraded products from the samples by gel filtration chromatography, and the purified samples migrated as a homogeneous band with over 95% purity when subjected to nonreducing SDS–PAGE analysis (Figure 4A). However, the two purified samples of aglycosylated FcγRIIIa and FcγRIIIa carrying one N-162 still contained a band with a relatively lower molecular weight than the intact products we had expected (Figure 4B). This unexpected band seemed to be FcγRIIIa with a nick or a small fragment deletion in the D2 domain because the band, which was also observed before gel filtration purification, had a comparable molecular weight of the intact product under nonreducing condition with the intact FcγRIIIa amino acid sequence (Figure 3). Interestingly, both the intact and derivative FcγRIIIa products showed a capability to bind IgG1 (Figure 5). The cleavage of the FcγRIIIa D2 domain at the lysine and arginine cluster region might not necessarily abolish the binding affinity to IgG antibodies.

In this study, we prepared a set of FcγRIIIa recombinants produced by CHO/DG44 cells, in which all of the attached oligosaccharides were of the complex type. Firstly, we confirmed that nonfucosylated antibody IgG1 shows significantly higher binding affinity to the fully glycosylated wild-type FcγRIIIa than does the fucosylated IgG1 and that this increased binding is almost abolished once all of the FcγRIIIa glycosylation is removed (Ferrara et al. 2006). Moreover, our gain-of-function analysis in the FcγRIIIa oligosaccharides also confirmed that N-162 is the element required for the high binding affinity to nonfucosylated antibodies and slightly reduces the affinity to fucosylated IgG1, as previously revealed by loss-of-function analyses (Galon et al. 1997; Drescher et al. 2003; Ferrara et al. 2006). It is worth noting that, beyond our expectation, the glycosylation at Asn-162 in FcγRIIIa significantly enhanced binding affinity to nonfucosylated IgG1 compared to the wild-type FcγRIIIa, and attachment of the other four oligosaccharides, especially N-45, hinders the high binding affinity to nonfucosylated IgG1. The crystal structure of aglycosylated FcγRIIIa, in complex with the Fc fragment of human IgG1, indicates that an oligosaccharide moiety at Asn-162 of FcγRIIIa could point into the central cavity within the Fc fragment (Sondermann et al. 2000), where the rigid core oligosaccharides attached to the Fc of IgG at Asn-297 are also located (Huber et al. 1976). The high affinity of antibodies lacking core fucosylation to FcγRIIIa is partially mediated by interactions formed between N-162 and regions of the Fc that are accessible only when the Fc oligosaccharide is nonfucosylated (Ferrara et al. 2006). Our data clearly demonstrated that the glycosylation at Asn-45 in FcγRIIIa reduces its high binding affinity mediated by N-162 to antibody IgG1 lacking core fucosylation. The conformational change of the D2 domain and the hinge region known to directly contact IgG (Sondermann et al. 2000) might be caused by N-45 modification of the FcγRIIIa D1 domain.

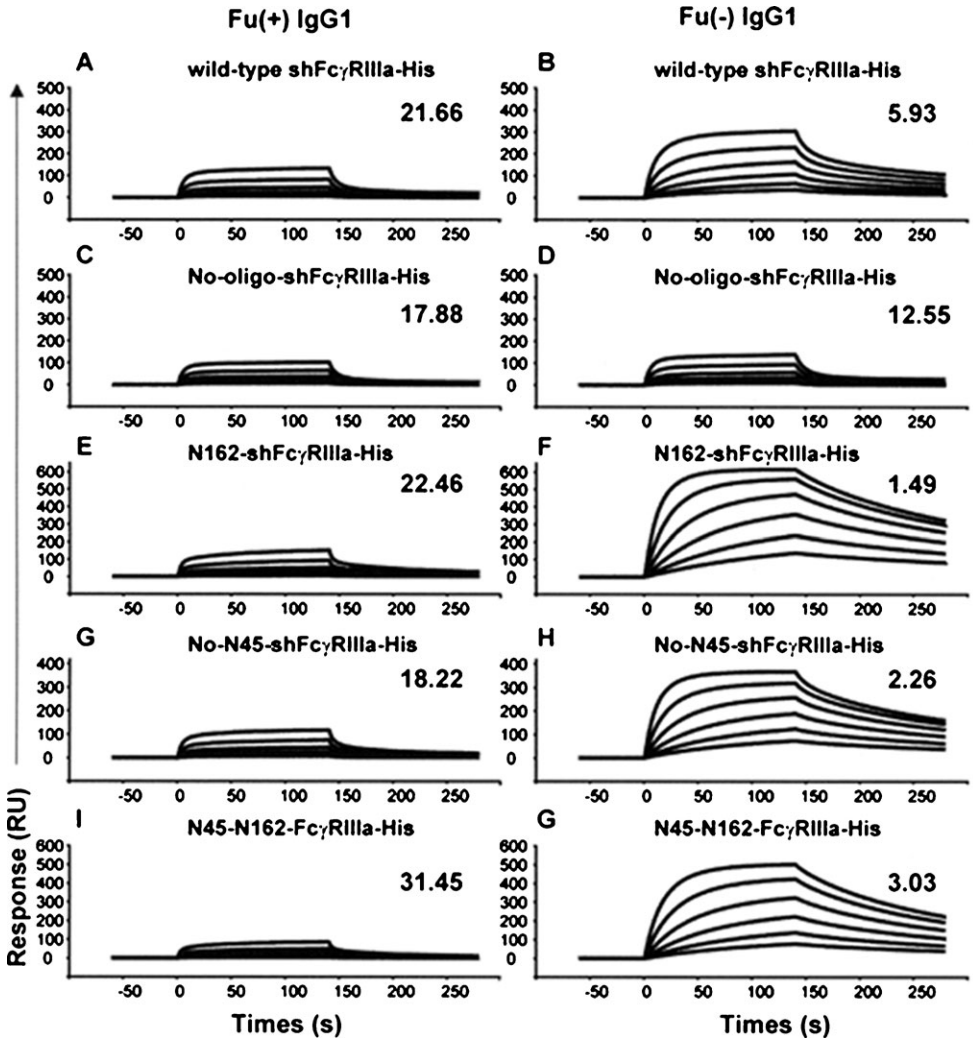

Fig. 8. Surface plasmon resonance analysis of shFcγRIIIa-His binding to IgG1. Fucosylated (Fu(+)) and nonfucosylated (Fu(−)) anti-CD20 IgG1s were injected over shFcγRIIIa-His (the wild-type shFcγRIIIa-His (**A** and **B**), No-oligo-shFcγRIIIa-His (**C** and **D**), N162-shFcγRIIIa-His (**E** and **F**), No-N45-shFcγRIIIa-His (**G** and **H**), N45-N162-shFcγRIIIa-His (**I** and **G**)) capture sensor chip at six different concentrations (ranging from 4.17 to 133.3 nM). In a control experiment, the buffer solution without IgG1 was injected over the receptor-capture sensor chip. The sensorgram obtained from the control experiment was subtracted from the sensorgrams obtained by the IgG1 injection to yield the curves presented in the figure. The dissociation constant (K_D: $\times 10^{-7}$ M) for the shFcγRIIIa-His calculated by steady-state analysis is shown on the right side on each sensorgram in the figure. The maximum value of the longitudinal axis was fitted to each predicted R_{max} value (maximum response).

Material and methods

Cell line

The CHO/DG44 cell line, in which the dihydrofolate reductase (DHFR) gene locus is deleted, was obtained from Drs. Lawrence Chasin and Gail Urlaub Chasin, Columbia University, New York (Urlaub et al. 1980). The CHO cell line was cultured in an IMDM medium (Invitrogen, Carlsbad, CA) containing 10% (v/v) dialyzed fetal bovine serum (dFBS; Invitrogen), 0.1 mM hypoxanthine, and 16 μM thymidine using a tissue culture flask (Greiner, Frickenhausen, Germany).

Antibodies

Mouse/human chimeric nonfucosylated and fucosylated anti-human CD20 IgG1s were generated as described previously (Yamane-Ohnuki et al. 2004; Iida et al. 2006). Rituximab (Rituxan®), purchased from Genentech, Inc. (South San Francisco, CA), was used for the controls. Table I shows the oligosaccharide structures of the Fc of each prepared IgG1, characterized by modified high-performance anion exchange chromatography (HPAEC) and matrix-assisted laser

Table I. Oligosaccharide analysis of the mouse/human chimeric anti-CD20 IgG1s

	Relative composition of oligosaccharides (%)[a]						
Antibody	G0	G1	G2	G0F	G1F	G2F	Fu(−)[b]
Nonfucosylated anti-CD20	64.0	33.0	3.0	n.d.[c]	n.d.	n.d.	100
Fucosylated anti-CD20	n.d.	n.d.	n.d.	41.9	51.1	7.0	n.d.
Rituximab	n.d.	n.d.	n.d.	55.1	40.8	4.1	n.d.

[a]Each composition value reflects the relative amount in the total complex-type oligosaccharides detected.
[b]Relative amount of nonfucosylated oligosaccharides.
[c]n.d.: not detected (less than 2.0%).

desorption/ionization time-of-flight mass spectrometry (MALDI-TOF MS) in positive-ion mode. Anti-human CD20s have an amino acid sequence equivalent to that of rituximab, which is widely used for the treatment of non-Hodgkin's lymphoma, and thus they exhibit identical binding activity to the specific antigen on antigen-binding ELISA and flow cytometric analyses, regardless of the Fc oligosaccharide structure (Iida et al. 2006). Antibodies were stored in a 0.01 M citrate buffer, pH 6.0, with 0.15 M NaCl. The concentration of purified antibodies was measured by absorbance at 280 nm.

Wild-type and oligosaccharide-depleted FcγRIIIa mutants

The hexa-His-tagged soluble human recombinant FcγRIIIa (shFcγRIIIa-His) was prepared as described previously (Niwa, Hatanaka, et al. 2004). Briefly, the cDNA encoding FcγRIIIa was isolated by reverse transcription-PCR (Superscript Preamplification System, Invitrogen) of oligo(dT)-primed RNA from human leukocyte 5′-stretch plus cDNA library (Clontech, Palo Alto, CA) using specific primers that generated the fragment encoding an extracellular domain, and the transmembrane and intracellular domains were replaced by DNA encoding a hexa-His-tag. Using PCR with specific primers, 5′-CGGAA TTCGCCTCCTCAAAATGAACCTCGGGCTCAGTTTGATT TTCCTTGCCCTCATTTTAAAAGGTGTCCAGTGTGAAGA TCTCCCAAAGGCTG-3′ and 5′-TCATCATTGACAGGATCC CG-3′, the N-terminal amino acid of the shFcγRIIIa-His was unified to Glu^3 (residue numbers excluding the signal peptide) by directly connecting to the signal peptide to avoid the N-terminal amino acid heterogeneity observed in the expression of original FcγRIIIa cDNA. Thus, the expected protein is composed of the extracellular domain of FcγRIIIa-Val-158 (a high-affinity FcγRIIIa allotype) linking hexa-His-tag at its C-terminus Gly-175. To mutate asparagine of the FcγRIIIa *N*-glycosylation sites into glutamine, a site-directed PCR mutagenesis kit (Stratagene, La Jolla, CA) was employed. The constructed cDNA fragments were inserted into a mammalian cell expression vector, pKANTEX93 (Nakamura et al. 2000), using the EcoRI and BamHI sites. The resultant vectors were transfected into CHO/DG44 by electroporation, and transfectants were selected in the IMDM medium containing 500 μg/mL of G418 without hypoxanthine or thymidine. The confluent transfectants were cultured in an Ex-Cell 301 medium (JRH Biosciences, Piscataway, NJ) in the presence or absence of protease inhibitor cocktail (Sigma-Aldrich, St. Louis, MO) and PMSF (Wako, Osaka, Japan) for 1 week, and the expressed proteins were purified from the culture supernatant by Ni-NTA chromatography (Qiagen, Valencia, CA) and gel filtration chromatography using an ÄKTA purifier (Amersham Biosciences, Piscataway, NJ). Samples equilibrated with a running buffer (0.15 M NaCl, 0.05 M NaH_2PO_4, pH 7.4) by a buffer exchange with Amicon Ultra (Millipore, Billerica, MA) were loaded onto Sephadex 75 10/300 GL (GE Healthcare, Uppsala, Sweden) at a flow rate of 0.5 mL/min. The purified proteins were stored in the running buffer, and the purified protein concentration was measured by absorbance at 280 nm. Their appropriate molecular weights were confirmed by SDS–PAGE (sample buffer: 62.5 mM Tris–acetate buffer, pH 6.5 containing 12.5% glycerol, 1% 2-ME, 2.5% SDS, and 0.005% bromphenol blue, gel: SDS–PAGE (Atto, Tokyo, Japan)). The purity of the products was estimated by SDS–PAGE analysis using a GS-800 calibrated densitometer (BioRad Laboratories, Hercules, CA).

N-Terminal amino acid sequence analysis

Samples were subjected to 12% SDS–PAGE analysis, followed by electroblotting onto a polyvinylidine difluoride (PVDF) membrane using a semidry blotting system (model AE-6675; Atto). Each band on the PVDF membrane was excised by a cutter and subjected to N-terminal amino acid sequencing via the Edman degradation method using a PPSQ-10 sequencer (Shimazu Co., Kyoto, Japan).

IgG affinity chromatography

Nonfucosylated anti-CD20 IgG1 (0.95 mg) was immobilized onto 0.4 mL of NHS-activated Sepharose 4 Fast Flow (GE Healthcare) according to the manufacturer's instructions. The IgG1-immobilized Sepharose was washed and equilibrated with 4 mL of running buffer, and 133 μg of purified N162-shFcγRIIIa-His (270 μL in running buffer) was loaded onto the column. After incubation at 4°C for 1 h, 400 μL of flowthrough fraction was collected. The adsorbed materials were eluted with a citrate-NaOH buffer, pH 4.0, after washing the column with 4 mL of the equilibration buffer. A sample (2 μg) of each fraction was subjected to SDS–PAGE analysis.

FcγRIIIa-derived N-linked oligosaccharide analysis

N-Linked oligosaccharides were released by digestion of the purified N162-shFcγRIIIa-His (60 μg) with two units of recombinant peptide-*N*-glycosidase F (PNGase F; Sigma-Aldrich) for 16 h at 37°C in 0.01 M Tris–acetate buffer, pH 8.3. The released oligosaccharides were recovered after precipitation of the protein with 75% ethanol. After the recovered supernatant was dried, the oligosaccharides were dissolved in 13 mM acetic acid and incubated at room temperature for 2 h. The acid-treated samples were desalted with cation-exchange resin (AG50W-X8, hydrogen form; BioRad Laboratories) and dried in vacuum. The dried samples were dissolved in deionized water and mixed with a matrix to be characterized by a MALDI-TOF MS spectrometer Reflex III (Bruker Daltonik GmbH, Bremen, Germany) equipped with delayed extraction. The released carbohydrates were analyzed both in a positive-ion mode using the super-DHB solution (Bruker Daltonik) as a matrix and in a negative-ion mode using 2′,4′,6′-trihydroxyacetophenon (THAP) as a matrix as described previously (Papac et al. 1996; Kanda et al. 2006).

IgG1-binding assay

The binding affinity of anti-CD20 IgG1 to each purified FcγRIIIa was measured by an FcγRIIIa-binding ELISA assay using plates coated with each shFcγRIIIa-His via anti-tetra-His antibodies (Qiagen) as described previously (Niwa, Hatanaka, et al. 2004). The binding kinetics of IgG1 to each of the purified shFcγRIIIa-His was measured using a T100 biosensor system instrument (BIAcore) as follows. Anti-tetra-His antibodies were immobilized onto the BIAcore sensor chip CM5 using an amine-coupling kit (BIAcore) according to the manufacturer's instructions. Each shFcγRIIIa-His was captured by the immobilized anti-tetra-His antibodies by the injection of shFcγRIIIa-His in a HBS-EP buffer (0.15 M NaCl, 3 mM EDTA, 0.005% Surfactant P20, 0.01 M HEPES, pH 7.4) at a flow rate of 5 μL/min.

The HBS-EP buffer lacking shFcγRIIIa-His was injected over the anti-tetra-His immobilized sensor surface; samples treated in this manner were used as a reference. The anti-CD20 IgG1 was diluted in the HBS-EP buffer at six different concentrations (ranging from 4.17 to 133.3 nM). Each diluted IgG1 was injected over the receptor-capture sensor surface at a flow rate of 30 μL/min. The experiments were performed at 25°C with the HBS-EP buffer as the running buffer. To obtain a blank control, the buffer solution lacking IgG1 was injected over the receptor-capture sensor surface. Prior to analysis, the data obtained by the injection of IgG1 were corrected for the reference and blank control. The dissociation constant (K_D) for each FcγRIIIa was calculated by steady-state analysis using the T100 biosensor system evaluation software version 1.0 (BIAcore). To repeat experiments, shFcγRIIIa-His and IgG1 were removed from the sensor tips by injection of 0.01 M Glycine–HCl, pH 1.5, at a flow rate of 60 μL/min for 1 min.

Conflict of interest statement

None declared.

Abbreviations

ADCC, antibody-dependent cellular cytotoxicity; CDC, complement-dependent cytotoxicity; CHO, Chinese hamster ovary; DHFR, dihydrofolate reductase; ELISA, enzyme-linked immunosorbent assay; HPAEC, high-performance anion exchange chromatography; IgG1, immunoglobulin G1; MALDI-TOF MS, matrix-assisted laser desorption/ionization time-of-flight mass spectrometry; NK, natural killer; PCR, polymerase chain reaction; PMSF, phenylmethylsulfonyl fluoride; PNGase F, peptide-*N*-glycosidase F; PVDF, polyvinylidine difluoride; SDS–PAGE, sodium dodecyl sulfate–polyacrylamide gel electrophoresis; THAP, 2′,4′,6′-trihydroxyacetophenon.

References

Anolik JH, Campbell D, Felgar RE, Young F, Sanz I, Rosenblatt J, Looney RJ. 2003. The relationship of FcgammaRIIIa genotype to degree of B cell depletion by rituximab in the treatment of systemic lupus erythematosus. *Arthritis Rheum.* 48:455–459.

Cartron G, Dacheux L, Salles G, Solal-Celigny P, Bardos P, Colombat P, Waitier H. 2002. Therapeutic activity of humanized anti-CD20 monoclonal antibody and polymorphism in IgG Fc receptor FcγRIIIa gene. *Blood.* 99:754–758.

Clark MR. 1997. IgG effector mechanisms. *Chem Immunol.* 65:88–110.

Dall'Ozzo S, Tartas S, Paintaud G, Carton G, Colonbat P, Bardos P, Watier H, Thibaut G. 2004. Rituximab-dependent cytotoxicity by natural killer cells: Influence of FCGR3A polymorphism on the concentration-effect relationship. *Cancer Res.* 64:4664–4669.

Dresher B, Witte T, Schimidt RE. 2003. Glycosylation of FcγRIII in N163 as mechanism of regulating receptor affinity. *Immunol.* 110:335–340.

Ferrara C, Stuart F, Sondermann P, Brunker P, Umana P. 2006. The carbohydrate at FcγRIIIa Asn-162: An element required for high affinity binding to non-fucosylated IgG glycoforms. *J Biol Chem.* 281:5032–5036.

Galon J, Robertson MW, Galinha A, Mazieres N, Spagnoli R, Fridman WF, Sautes C. 1997. Affinity of the interaction between Fc gamma receptor type III (FcγRIIIa) and monomeric human IgG subclasses. Role of FcγRIII glycosylation. *Eur J Immunol*. 27:1928–1932.

Gennari R, Menard S, Fagnoni F, Ponchio L, Scelsi M, Tagliabue E, Castiglioni F, Villani L, Magalotti M, Gibelli N, et al. 2004. Pilot study of the mechanism of action of preoperative trastuzumab in patients with primary operable breast tumors overexpressing HER2. *Clin Cancer Res.* 10:5650–5655.

Harris LJ, Skaletsky E, Mcpherson A. 1998. Crystallographic structure of an intact IgG1 monoclonal antibody. *J. Mol. Biol.* 275:861–872.

Huber R, Deisenhofer J, Colman PM. 1976. Crystallographic structure studies of an IgG molecule and an Fc fragment. *Nature.* 264:415–420.

Iida S, Misaka H, Inoue M, Sibata M, Nakano R, Yamane-Ohnuki N, Wakitani M, Yano K, Shitara K, Satoh M. 2006. Non-fucosylated therapeutic IgG1 antibody can evade the inhibitory effect of serum IgG on antibody-dependent cellular cytotoxicity through its high binding to FcγRIIIa. *Clin Cancer Res.* 12(9):2879–2887.

Kanda Y, Yamada T, Mori K, Okazaki A, Inoue M, Kitajima-Miyama K, Kuni-Kamochi R, Nakano R, Yano K, Kakita S, et al. 2006. Comparison of biological activity among nonfucosylated therapeutic IgG1 antibodies with three different *N*-linked Fc oligosaccharides: The high-mannose, hybrid, and complex types. *Glycobiology.* 17:104–118.

Kim DH, Jung HD, Kim JG, Lee JJ, Yang DH, Park YH, Do YR, Shin HJ, Kim MK, Hyun MS, et al. 2006. FCGR3A gene polymorphisms may correlate with response to frontline R-CHOP therapy for diffuse large B-cell lymphoma. *Blood.* 108:2720–2725.

Krapp S, Mimura Y, Jefferis R, Huber R, Sondermann PJ. 2003. Structural analysis of human IgG-Fc glycoforms reveals a correlation between glycosylation and structural integrity. *Mol Biol.* 325:979–989.

Louis E, El Ghoul Z, Vermeire S, Dall'Ozzo S, Rutgeerts P, Paintaud G, Belaiche J, De Vos M, Van Gossum A, Colombel JF, et al. 2004. Association between polymorphism in IgG Fc receptor IIIa coding gene and biological response to infliximab in Crohn's disease. *Aliment Pharmacol Ther.* 19:511–519.

Matsumiya S, Yamaguchi Y, Saito J, Nagano M, Sasakawa H, Otaki S, Satoh M, Shitara K, Kato K. 2007. Structural comparison of fucosylated and nonfucosylated Fc fragments of human immunoglobulin G1. *J Mol Biol.* 368(3):767–779.

Miescher S, Spycher MO, Amstutz H, De Haas M, Kleijer M, Kalus UJ, Radtke H, Hubsch A, Andresen I, Martin RM, et al. 2004. A single recombinant anti-RhD IgG prevents RhD immunization: Association of RhD-positive red blood cell clearance rate with polymorphisms in the FcγRIIA and FcγIIIA genes. *Blood.* 103:4028–4035.

Morgan A, Jones ND, Nesbitt AM, Chaplin L, Bodmer MW, Emtage JS. 1995. The N-terminal end of the CH2 domain of chimeric human IgG1 anti-HLA-DR is necessary for Ci1q, FcRI and FcRIII binding. *Immunology.* 86:319–324.

Nakanuma K, Tanaka Y, Fujino I, Hirayama N, Shitara K, Hanai N. 2000. Dissection and optimization of immune effector function of humanized anti-ganglioside GM2 monoclonal antibody. *Mol Immunol.* 37:1035–4106.

Niwa R, Hatanaka S, Shoji-Hosaka E, Sakurada M, Kobayashi Y, Uehara A, Yokoi H, Nakamura K, Shitara K. 2004. Enhancement of the antibody-dependent cellular cytotoxicity of low-fucose IgG1 is independent of FcγRIIIa functional polymorphism. *Clin Cancer Res.* 10:6248–6255.

Niwa R, Sakurada M, Kobayashi Y, Uehara A, Matsushima K, Ueda R, Nakamura K, Shitara K. 2005. Enhanced natural killer cell binding and activation by low-fucose IgG1 antibody results in potent antibody-dependent cellular cytotoxicity induction at lower antigen density. *Clin Cancer Res.* 11:2327–2336.

Niwa R, Shoji-Hosaka E, Sakurada M, Uchida K, Nakamura K, Matsushima K, Ueda R, Hanai N, Shitara K. 2004. Defucosylated chimeric anti-CC chemokine receptor 4 IgG1 with enhanced antibody-dependent cellular cytotoxicity shows potent therapeutic activity to T-cell leukemia and lymphoma. *Cancer Res.* 64:2127–2133.

Okazaki A, Shoji-Hosaka E, Nakamura K, Wakitani M, Uchida K, Kakita S, Tsumato K, Kumagai I, Shitara K. 2004. Fucose depletion from human IgG1 oligosaccharide enhances binding enthalpy and association rate between IgG1 and FcγRIIIa. *J Mol Biol.* 336:1239–1249.

Papac D, Wong A, Jones AJ. 1996. Analysis of acidic oligosaccharides and glycopeptides by matrix-assisted laser desorption/ionization time-of-flight mass spectrometry. *Anal Chem.* 68:3215–3223.

Radaev S, Motyka S, Fridman W, Sautes-Fridman C, Sun PD. 2001. The structure of a human type III Fcγ receptor in complex with Fc. *J Biol Chem.* 276:16469–16477.

Ravetch JV, Perussia B. 1989. Alternative membrane forms of FcγRIII (CD16) on human natural killer cells and neutrophils. *J Exp Med.* 170:481–497.

Satoh M, Iida S, Shitara K. 2006. Non-fucosylated therapeutic antibodies as next-generation therapeutic antibodies. *Exp Opin Biol Ther.* 6:1161–1173.

Shields RL, Lai J, Keck R, O'connell LY, Hong K, Meng YG, Weikert SH, Presta LG. 2002. Lack of fucose on human IgG1 *N*-linked oligosaccharide improves binding to human FcγRIII and antibody-dependent cellular toxicity. *J Biol Chem.* 277:26733–26740.

Shinkawa T, Nakamura K, Yamane N, Shoji-Hosaka E, Kanda Y, Sakurada M, Uchida K, Anazawa H, Satoh M, Yamasaki M, et al. 2003. The absence of fucose but not the presence of galactose or bisecting *N*-acetylglucosamine of human IgG1 complex-type oligosaccharides shows the critical role of enhancing antibody-dependent cellular cytotoxicity. *J Biol Chem.* 278:3466–3673.

Sondermann P, Huber R, Oosthyzen V, Lacob U. 2000. The 3.2-A crystal structure of the human IgG1 Fc fragment-Fc gammaRIII complex. *Nature.* 406:267–273.

Suzuki A, Niwa R, Saji S, Muta M, Hirose M, Iida S, Shiotsu Y, Satoh M, Shitara K, Kondo M, et al. 2007. A nonfucosylated anti-HER2 antibody augments antibody-dependent cellular cytotoxicity in breast cancer patients. *Clin Cancer Res.* 13:1875–1882.

Treon SP, Hansen M, Branagan AR, Verselis S, Emmanouilides C, Kimby E, Frankel SR, Touroutoglou N, Turnbull B, Anderson KC, et al. 2005. Polymorphisms in FcγRIIIA (CD16) receptor expression are associated with clinical response to rituximab in Waldenström's macroglobulinemia. *J Clin Oncol.* 23:474–481.

Urlaub G, Chasin LA. 1980. Isolation of Chinese hamster cell mutants deficient in dihydrofolate reductase activity. *Proc Natl Acad Sci USA*.77:4216–4220.

Weng WK, Levy R. 2003. Two immunoglobulin G fragment C receptor polymorphisms independently predict response to rituximab in patients with follicular lymphoma. *J Clin Oncol.* 21:3940–3947.

Yamane-Ohnuki N, Kinoshita S, Inoue-Urakubo M, Kusunoki M, Iida S, Nakano R, Wakitani M, Niwa R, Sakurada M, Uchida K, et al. 2004. Establishment of *FUT8* knockout Chinese hamster ovary cells: An ideal host cell line for producing completely defucosylated antibodies with enhanced antibody-dependent cellular cytotoxicity. *Biotechnol Bioeng.* 87:614–622.